

# Linear $X$ -wave generation by means of cross-phase modulation in Kerr media

A. Averchi,<sup>1,6,\*</sup> D. Faccio,<sup>1,6</sup> E. Rubino,<sup>1,6</sup> H. Valtna Lukner,<sup>2,3</sup> P. Panagiotopoulos,<sup>4</sup> P. A. Loukakos,<sup>4</sup>  
S. Tzortzakis,<sup>4</sup> A. Couairon,<sup>5,6</sup> and P. Di Trapani<sup>1,3,6</sup>

<sup>1</sup>Department of Physics and Mathematics, CNISM University of Insubria, Via Valleggio 11, IT-22100 Como, Italy

<sup>2</sup>Institute of Physics, University of Tartu, Riia 142, 51014 Tartu, Estonia

<sup>3</sup>Department of Quantum Electronics, Vilnius University, Sauletekio Avenue 9, Building 3,  
LT-10222 Vilnius, Lithuania

<sup>4</sup>Institute of Electronic Structure and Laser, Foundation for Research and Technology-Hellas (IESL-FORTH),  
P.O. Box 1527, 711110 Heraklion, Greece

<sup>5</sup>Centre de Physique Théorique, CNRS, École Polytechnique, F-91128 Palaiseau, France

<sup>6</sup>Virtual Institute for Nonlinear Optics, Centro di Cultura Scientifica Alessandro Volta, Villa Olmo,  
Via Simone Cantoni 1, 22100 Como, Italy

\*Corresponding author: [alessandro.averchi@uninsubria.it](mailto:alessandro.averchi@uninsubria.it)

Received July 25, 2008; accepted October 3, 2008;

posted November 17, 2008 (Doc. ID 99407); published December 12, 2008

We exploit cross-phase modulation by a strong driving pulse onto a weaker probe pulse at a different wavelength to induce the formation of an  $X$  wave possessing the typical nondispersive and nondiffractive propagation properties. © 2008 Optical Society of America  
OCIS codes: 190.7110, 320.2250.

$X$  waves belong to the wider class of so-called “conical waves,” i.e., wave packets in which the energy flow is not axial but is directed along a cone centered around the propagation axis. All conical waves share the property of being nondiffractive (experimentally, over a finite distance), but only  $X$  waves are able to achieve also nondispersive propagation in dispersive media [1], thanks to their angular dispersion that also determines the  $X$ -wave group velocity, which is in general different from that of a Gaussian pulse centered at the same wavelength. Among other systems, spontaneous  $X$ -wave formation has been predicted and extensively studied in the process of optical pulse filamentation in Kerr media [2–4], which is a spatiotemporal dynamic reshaping of the pulse driven by nonlinear effects in the medium manifested as the formation of a high intensity core propagating over long distances without spreading [5]. Recently, in the context of “two-color filamentation” studies—where the filamenting pulse copropagates with a pulse at a different wavelength— $X$ -wave formation induced by filaments has been reported in [6,7]. In the presence of stimulated Raman scattering (SRS) the reshaping of a Gaussian seed into an  $X$  wave and its subsequent amplification by SRS were investigated. In this interaction, cross-phase modulation (XPM) was found to be responsible for seed reshaping. Its effect can be described as a scattering potential that drives the probe to travel at the same group velocity of the filament by transforming it into an  $X$  wave.

In this Letter for the first time (to our knowledge) we experimentally study in detail the effect of XPM in the absence of energy transfer between a filament (1055 nm) and a weak probe pulse (527 nm) in conditions similar to those simulated in [8]. We observe that XPM induces on the probe a reshaping into a linear  $X$  wave that travels at the same group velocity as

the filament. As the  $X$  wave is well spectrally isolated, we filter out the filament at the end of the sample and characterize the propagation of the  $X$  wave alone in air, which shows remarkable nondiffracting properties. Moreover we show that, as long as the XPM-inducing pulse maintains a high intensity over a long propagation distance, a filament is not strictly necessary to induce the  $X$ -wave reshaping; to this purpose we repeat the experiment using a Bessel pulse as the driving pulse.

Experiments in the filamentation regime were carried out using 1.2 ps duration (FWHM) 1055 nm laser pulses delivered by a 10 Hz amplified Nd:glass laser. The beam was split into two by means of a 50/50 beam splitter. On one arm the 527 nm pulse was generated by frequency doubling the fundamental pulse with a potassium diphosphate crystal beyond which a variable delay line was mounted. The green and IR pulses were then recombined with an IR high reflectivity dielectric mirror and focused with an  $f=50$  cm lens (as in [6,7]) to a diameter of 100  $\mu\text{m}$  onto the input facet of a 2-cm-long long fused silica sample. The energies of the two pulses ( $E_{\text{pump}}, E_{\text{probe}}$ ) were controllable independently by first-order half-wave plates and polarizers. The absence of energy transfer from the filament to the green pulse was experimentally verified by measuring the energy of the green pulse before and after the sample with a power meter (OPHIR, Nova).

In Fig. 1 we show the angularly resolved ( $\theta, \lambda$ ) spectrum of the 527 nm pulse measured with an imaging spectrometer (Lot-Oriel, MS260i) after the sample and recorded with a digital Nikon D70 camera. In Fig. 1(a) the IR pulse was blocked, and the weak green pulse was let to propagate alone inside the sample; as expected the intensity profile in the spectrum is Gaussianlike. In Fig. 1(b) the filamenting IR pulse ( $E_{\text{pump}}=20 \mu\text{J}$ ) was spatially and tempo-

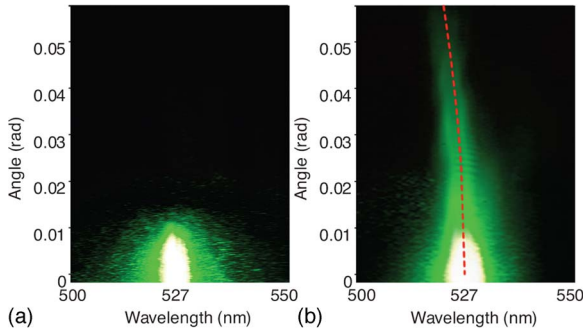


Fig. 1. (Color online)  $(\theta, \lambda)$  Spectrum of the 527 nm probe pulse after the sample (a) when the IR pulse is blocked and (b) when the IR filamenting pulse is copropagating with the probe in the sample. XPM induces the formation of conical structures on the probe spectrum. The dashed curve is the plot of Eq. (1), describing the  $X$ -wave shape with the experimental group velocity of the  $X$  wave ( $v_x$ ) deduced from the spectrum of the filament as described in [7].

rally superimposed to the central portion of the green pulse ( $E_{\text{probe}} = 0.5 \mu\text{J}$ ). Although in the absence of any energy transfer from the filament, the green seed pulse clearly reshapes and develops conical tails, which in the angularly resolved spectrum are the well-known signature of  $X$ -wave formation [9].

To prove the genuine  $X$ -wave nature of this object, however, it is necessary to show its nondispersive and nondiffracting propagation. To demonstrate the first, in Fig. 1(b) we fit the spectrum using the  $X$ -wave relation that, for a given material and central wavelength, describes in the  $(\theta, \lambda)$  spectrum the loci, where the angular dispersion is able to compensate the material dispersion. In  $(k_{\perp}, \omega)$  coordinates—equivalent to  $(\theta, \lambda)$ —this relation takes the simple form [7]

$$k_z(\omega) = k(\omega_0) + \frac{\omega - \omega_0}{v_x}, \quad (1)$$

where  $\omega_0$  is a reference central frequency and  $k_{\perp}(\omega) = \sqrt{k(\omega)^2 - k_z(\omega)^2}$  and  $v_x$  is the group velocity of the  $X$  wave. As can be seen in Fig. 1(b), the curve matches very closely the experimental shape. We underline that this simple spectral intensity characterization is sufficient to prove that the pulse propagates without dispersing within the glass sample as, indeed, for a given medium; pulse spreading along the propagation direction is completely determined by the pulse dispersion relation  $k_z = k_z(\omega)$ . We note also that in our fit the group velocity of the  $X$  wave is not a free parameter; indeed, it is the group velocity of the driving pulse measured experimentally using the method described in detail in [7] and yielding  $v_x = 2.22 \pm 0.03 \times 10^8$  m/s. This allows us to confirm experimentally the prediction made in [7,8] that the  $X$  wave induced by XPM travels at the same group velocity as the driving pulse.

We then verified the nondiffracting propagation of the  $X$ -reshaped green pulse. To demonstrate this we simply let the two pulses propagate out of the sample in air, where the nonlinear refractive index is about

1000 times smaller than in silica, thus quenching the filament and all nonlinear effects. We then removed the IR light with a low-pass filter and scanned the green beam profile along its propagation in air, starting from the output facet of the sample. Our imaging system was composed by a lens and a 12-bit CCD camera (DTA iCam 400 E).

In Fig. 2(a) the normalized intensity profile of the probe at the output facet of the sample is shown. The effect of XPM from the filament is evident, with the formation of a narrow (7.8  $\mu\text{m}$ ) FWHM central peak surrounded by slowly decaying tails. We could fit its radial intensity profile with a rational function having the form  $a/(br^2 + cr)$ , which agrees well with the  $1/r^2$  decay for large radii expected for a linear  $X$  wave [10]. In Fig. 2(d) the measured FWHM of the beam profile along the  $z$  axis is shown. As can be seen, the central peak propagates nondiffractively, keeping its FWHM constant within the experimental error for a distance of about 5 mm, and then diffracts abruptly. This behavior at the end of the nondiffracting zone is typical of all the experimental realizations of conical waves and is due to the finite energy contained in the conical wave packet. Notably, on the same distance of 5 mm a collimated Gaussian beam with the same initial diameter would have reached a FWHM of about 120  $\mu\text{m}$ .

We performed a complementary experiment using a pulsed Bessel beam (PBB) instead of the filament as the driving pulse. Here our driving pulse was a 1 mJ, 35 fs pulse positively chirped to 1 ps (to optimize pump and seed temporal overlap) at 800 nm from an amplified Ti:sapphire laser system. The

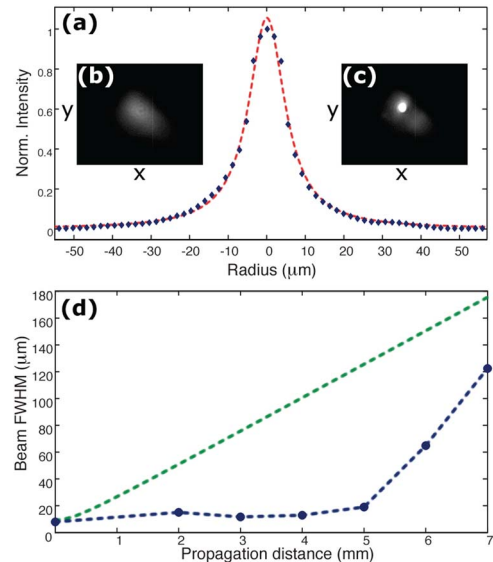


Fig. 2. (Color online) (a) Normalized intensity profile of the probe at the output of the sample in the presence of XPM. The dashed curve is the fit of the profile with a rational quadratic function. In the insets the near field of the green pulse is acquired with the CCD system (b) without XPM and (c) with XPM. Note that the probe energy was unchanged between the two measurements. (d) Probe beam FWHM along propagation after the sample (dashed curve with solid circles), nondiffracting over 5 mm. The theoretically predicted broadening for a Gaussian beam with the same FWHM is shown for comparison (dashed curve).

probe pulse was generated by frequency doubling with a  $\beta$ -barium borate crystal. The setup scheme was conceptually the same as the first experiment, with the addition of a 175 apex angle axicon mounted onto the IR beam line to reshape the driving pulse into a Bessel beam.

As we show in Fig. 3(a), the probe pulse—as expected—developed  $X$  wave tails in the  $(\theta, \lambda)$  spectrum due to XPM. We also performed a series of numerical simulations to confirm the validity of this last experimental result, using a code described in detail in [5]. In Fig. 3 the numerically predicted  $(\theta, \lambda)$  spectra of the probe pulse with and without XPM reshaping are reported. As may be seen, the numerics confirm our experimental findings. We note that the driving Bessel pulse suffered no significant changes owing to self-induced nonlinear effects as verified both numerically and experimentally (data not shown); i.e., no spectral broadening was observed. These last results confirm that the XPM reshaping of the probe pulse into an  $X$  wave is not necessarily related to filamentation of the pump pulse. Indeed Eq. (1) is derived under the sole assumption that the scattering polarization is localized in space (allowing the probe spectrum to spread in angle) and in time (allowing the probe to spread its temporal spectrum) [3].

In conclusion, in this Letter we have studied in detail the spatiotemporal reshaping induced by XPM from an intense driving pulse on a weaker probe at a different wavelength in a bulk Kerr medium. We

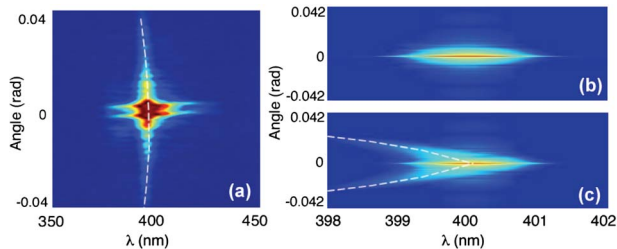


Fig. 3. (Color online) (a) Experimentally measured  $(\theta, \lambda)$  spectrum for the probe pulse at 400 nm reshaped by XPM driven from a PBB at 800 nm. The white curve is the  $X$ -wave relation curve calculated with Eq. (1), where  $v_x = 2.043 \times 10^8$  m/s is the theoretically predicted group velocity for the PBB. Numerically simulated  $(\theta, \lambda)$  spectrum for the probe pulse (b) before interaction with the driving pulse and (c) with XPM induced by the PBB.

have shown that XPM can be exploited to generate spectrally isolated linear  $X$  waves that propagate over a finite distance with no dispersion and no diffraction. Moreover we have shown the generality of this mechanism, which holds as long as the driving pulse propagates for a distance long enough with a sufficient intensity. We think that these results will be useful both as a tool to better understand current studies on two-color systems in the field of ultrashort nonlinear optics and to provide a feasible method to generate  $X$  waves in the optical domain.

The authors acknowledge support from CNSIM, project INNESCO, from the Lithuanian Science and Technology Foundation project ConTeX, from Marie Curie Chair project STELLA, contract MEXC-CT-2005-025710, and Marie Curie Excellence grant MULTI-RAD MEXT-CT-2006-042683. H. V. Lukner acknowledges support from the Sixth European Union (EU) Framework Program (ATLAS), contract MEST-CF-2004-008048. The results have been partly obtained during the STELLA school 2008 ([www.vino-stella.eu](http://www.vino-stella.eu)).

## References

1. H. Sonajalg and P. Saari, *Opt. Lett.* **15**, 1163 (1996).
2. C. Conti, S. Trillo, P. Di Trapani, G. Valiulis, A. Piskarskas, O. Jedrkiewicz, and J. Trull, *Phys. Rev. Lett.* **90**, 170406 (2003).
3. D. Faccio, M. A. Porras, A. Dubietis, F. Bragheri, A. Couairon, and P. Di Trapani, *Phys. Rev. Lett.* **96**, 193901 (2006).
4. M. Kolesik, E. M. Wright, and J. V. Moloney, *Phys. Rev. Lett.* **92**, 253901 (2004).
5. A. Couairon and A. Mysyrowicz, *Phys. Rep.* **441**, 47 (2007).
6. D. Faccio, A. Averchi, A. Dubietis, P. Polesana, A. Piskarskas, P. Di Trapani, and A. Couairon, *Opt. Lett.* **32**, 184 (2007).
7. D. Faccio, A. Averchi, A. Couairon, M. Kolesik, J. V. Moloney, A. Dubietis, G. Tamosauskas, P. Polesana, A. Piskarskas, and P. Di Trapani, *Opt. Express* **15**, 13077 (2007).
8. M. Kolesik and J. V. Moloney, *Opt. Express* **16**, 2971 (2008).
9. D. Faccio, P. Di Trapani, S. Minardi, A. Bramati, F. Bragheri, C. Liberale, V. Degiorgio, A. Dubietis, and A. Matijosius, *J. Opt. Soc. Am. B* **22**, 862 (2005).
10. J. Lu and J. F. Greenleaf, *IEEE Trans. Ultrason. Ferroelectr. Freq. Control* **39**, 19 (1992).